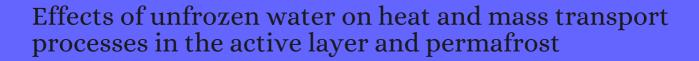
CITATION REPORT List of articles citing



DOI: 10.1002/1099-1530(200007/09)11:33.0.co;2-7 Permafrost and Periglacial Processes, 2000, 11, 219-239.

Source: https://exaly.com/paper-pdf/31574942/citation-report.pdf

Version: 2024-04-20

This report has been generated based on the citations recorded by exaly.com for the above article. For the latest version of this publication list, visit the link given above.

The third column is the impact factor (IF) of the journal, and the fourth column is the number of citations of the article.

#	Paper	IF	Citations
309	Quantifying the thermal dynamics of a permafrost site near Ny-Lesund, Svalbard. 2001, 37, 2901-2914		75
308	The first 20 years (1978-1979 to 1998-1999) of active-layer development, Illisarvik experimental drained lake site, western Arctic coast, Canada1. 2002 , 39, 1657-1674		55
307	Intraseasonal variation in the thermoinsulation effect of snow cover on soil temperatures and energy balance. 2002 , 107, ACL 13-1-ACL 13-6		53
306	Temperature controls of microbial respiration in arctic tundra soils above and below freezing. 2002 , 34, 1785-1795		391
305	Climate and the limits of permafrost: a zonal analysis. <i>Permafrost and Periglacial Processes</i> , 2002 , 13, 1-15	4.2	219
304	The mean annual temperature at the top of permafrost, the TTOP model, and the effect of unfrozen water. <i>Permafrost and Periglacial Processes</i> , 2002 , 13, 137-143	4.2	25
303	Impact of the timing and duration of seasonal snow cover on the active layer and permafrost in the Alaskan Arctic. <i>Permafrost and Periglacial Processes</i> , 2003 , 14, 141-150	4.2	92
302	A model for regional-scale estimation of temporal and spatial variability of active layer thickness and mean annual ground temperatures. <i>Permafrost and Periglacial Processes</i> , 2003 , 14, 125-139	4.2	86
301	Establishing long-term permafrost observatories for active-layer and permafrost investigations in Alaska: 1977\(\bar{2}\) 002. Permafrost and Periglacial Processes, 2003, 14, 331-342	4.2	40
300	Impacts of wildfire on the permafrost in the boreal forests of Interior Alaska. 2003, 108, FFR 4-1		191
299	Soil organic carbon and CO2 respiration at subzero temperature in soils of Arctic Alaska. 2003 , 108, ALT 5-1		86
298	Frozen soil parameterization in SiB2 and its validation with GAME-Tibet observations. 2003, 36, 165-187	2	61
297	Five Stages of the Alaskan Arctic Cold Season with Ecosystem Implications. 2003, 35, 74-81		78
296	Increased snow depth affects microbial activity and nitrogen mineralization in two Arctic tundra communities. 2004 , 36, 217-227		464
295	A numerical model for surface energy balance and thermal regime of the active layer and permafrost containing unfrozen water. 2004 , 38, 1-15		107
294	Comparing electronic probes for volumetric water content of low-density feathermoss. 2005 , 25, 215-2	21	9
293	Recent trends from Canadian permafrost thermal monitoring network sites. <i>Permafrost and Periglacial Processes</i> , 2005 , 16, 19-30	4.2	127

(2007-2005)

292	Soil water storage and active-layer development in a sub-alpine tundra hillslope, southern Yukon Territory, Canada. <i>Permafrost and Periglacial Processes</i> , 2005 , 16, 369-382	59
291	Changing microbial substrate use in Arctic tundra soils through a freeze-thaw cycle. 2005 , 37, 1411-1418	153
2 90	Evidence and Implications of Recent Climate Change in Northern Alaska and Other Arctic Regions. 2005 , 72, 251-298	1074
289	Freezing of Subarctic Hillslopes, Wolf Creek Basin, Yukon, Canada. 2005 , 37, 1-10	32
288	Reconstructing solid precipitation from snow depth measurements and a land surface model. 2005 , 41,	19
287	Permafrost Hydrology. 2005 ,	О
286	Winter Biological Processes Could Help Convert Arctic Tundra to Shrubland. 2005 , 55, 17	473
285	Long-term evaluation of the Hydro-Thermodynamic Soil-Vegetation Scheme's frozen ground/permafrost component using observations at Barrow, Alaska. 2006 , 111,	28
284	Hydrothermal regimes of the dry active layer. 2006 , 42,	23
283	Evaluation of the Soil Model of the HydroThermodynamic SoilNegetation Scheme by Observations and a Theoretically Advanced Numerical Scheme. 2006 , 134, 2927-2942	1
282	Microbial activity in soils frozen to below 🖰 9 🖒 2006, 38, 785-794	179
281	Soil microbial and nutrient dynamics in a wet Arctic sedge meadow in late winter and early spring. 2006 , 38, 2843-2851	122
280	Cold-season Production of CO2 in Arctic Soils: Can Laboratory and Field Estimates Be Reconciled through a Simple Modeling Approach?. 2006 , 38, 249-256	45
279	What determines the current presence or absence of permafrost in the TornetrEk region, a sub-arctic landscape in northern Sweden?. 2006 , 35, 190-7	66
278	Responses of springtail and mite populations to prolonged periods of soil freeze-thaw cycles in a sub-arctic ecosystem. 2007 , 36, 136-146	75
277	Past and recent changes in air and permafrost temperatures in eastern Siberia. 2007 , 56, 399-413	128
276	Three-dimensional distribution and evolution of permafrost temperatures in idealized high-mountain topography. 2007 , 112,	152
275	Evaluating a high-resolution climate model: Simulated hydrothermal regimes in frozen ground regions and their change under the global warming scenario. 2007 , 112,	59

274	Characteristics of the recent warming of permafrost in Alaska. 2007, 112,	198
273	Conservation of soil organic matter through cryoturbation in arctic soils in Siberia. 2007, 112,	101
272	Improved modeling of permafrost dynamics in a GCM land-surface scheme. 2007, 34,	152
271	Using in-situ temperature measurements to estimate saturated soil thermal properties by solving a sequence of optimization problems. 2007 , 1, 41-58	29
270	A simple heat-conduction method for simulating the frost-table depth in hydrological models. 2007 , 21, 2610-2622	81
269	Groundwater flow with energy transport and waterite phase change: Numerical simulations, benchmarks, and application to freezing in peat bogs. 2007 , 30, 966-983	171
268	Annual soil CO2 effluxes in the High Arctic: The role of snow thickness and vegetation type. 2007 , 39, 646-654	102
267	Plant Species Composition and Productivity following Permafrost Thaw and Thermokarst in Alaskan Tundra. 2007 , 10, 280-292	183
266	Soil microbial activity along an arctic-alpine altitudinal gradient from a seasonal perspective. 2008 , 59, 842-854	24
265	Evaluation of the algorithms and parameterizations for ground thawing and freezing simulation in permafrost regions. 2008 , 113,	74
264	Advances in the continuous monitoring of erosion and deposition dynamics: Developments and applications of the new PEEP-3T system. 2008 , 93, 17-39	39
263	Arctic land hydrothermal sensitivity under warming: Idealized off-line evaluation of a physical terrestrial scheme in a global climate model. 2008 , 113,	11
262	Effects of Simulated Climate Change on Plant Phenology and Nitrogen Mineralization in Alaskan Arctic Tundra. 2008 , 40, 27-38	76
261	Multi-offset GPR methods for hyporheic zone investigations. 2009 , 7, 247-257	8
260	Transient thermal effects in Alpine permafrost. 2009 , 3, 85-99	97
259	THM-coupled finite element analysis of frozen soil: formulation and application. 2009, 59, 159-171	133
258	Microbial Activity in Frozen Soils. 2009 , 119-147	16
257	Exponential growth of anow molds at sub-zero temperatures: an explanation for high beneath-snow respiration rates and Q 10 values. 2009 , 95, 13-21	42

(2010-2009)

256	Experimental study on the physical-mechanical properties of frozen silt. 2009 , 13, 317-324		19
255	Hydrothermal pattern of frozen soil in Nam Co lake basin, the Tibetan Plateau. 2009 , 57, 1775-1784		18
254	Water availability controls microbial temperature responses in frozen soil CO2 production. 2009 , 15, 2715-2722		92
253	Mathematical modeling of the atmosphere-cryolitic zone interaction. 2009 , 45, 687-703		3
252	Estimation of soil thermal properties using in-situ temperature measurements in the active layer and permafrost. 2009 , 55, 120-129		70
251	Ultrasonic technique as tool for determining physical and mechanical properties of frozen soils. 2009 , 58, 136-142		41
250	Contributions of matric and osmotic potentials to the unfrozen water content of frozen soils. 2009 , 148, 392-398		41
249	Chemical and isotopic characterization of size-fractionated organic matter from cryoturbated tundra soils, northern Alaska. 2009 , 114,		50
248	The Effect of Moisture Content on the Thermal Conductivity of Moss and Organic Soil Horizons From Black Spruce Ecosystems in Interior Alaska. 2009 , 174, 646-651		118
247	Permafrost thermal state in the polar Northern Hemisphere during the international polar year 2007 2009: a synthesis. <i>Permafrost and Periglacial Processes</i> , 2010 , 21, 106-116	4.2	506
246	Meltwater infiltration into the frozen active layer at an alpine permafrost site. <i>Permafrost and Periglacial Processes</i> , 2010 , 21, 325-334	4.2	77
245	Decomposition of old organic matter as a result of deeper active layers in a snow depth manipulation experiment. 2010 , 163, 785-92		89
244	Is the decline of soil microbial biomass in late winter coupled to changes in the physical state of cold soils?. 2010 , 42, 129-135		91
243	Unfrozen water content moderates temperature dependence of sub-zero microbial respiration. 2010 , 42, 1396-1407		45
242	Frozen soil parameterization in a distributed biosphere hydrological model. 2010 , 14, 557-571		56
241	Permafrost Weakening as a Potential Impact of Climatic Warming. 2010 , 24, 1-18		8
240	Phosphorus Solubilization and Potential Transfer to Surface Waters from the Soil Microbial Biomass Following DryingRewetting and FreezingThawing. 2010 , 106, 1-35		93
239	Decadal variations of active-layer thickness in moisture-controlled landscapes, Barrow, Alaska. 2010 , 115,		118

238	Effects of soil organic matter composition on unfrozen water content and heterotrophic CO2 production of frozen soils. 2010 , 74, 2281-2290		17
237	Permafrost response to last interglacial warming: field evidence from non-glaciated Yukon and Alaska. 2010 , 29, 3256-3274		59
236	Resilience and vulnerability of permafrost to climate changeThis article is one of a selection of papers from The Dynamics of Change in Alaska Boreal Forests: Resilience and Vulnerability in Response to Climate Warming 2010 , 40, 1219-1236		345
235	Thermal modeling of roadway embankments over permafrost. 2011 , 65, 474-487		23
234	Exploring the sensitivity of soil carbon dynamics to climate change, fire disturbance and permafrost thaw in a black spruce ecosystem. 2011 , 8, 1367-1382		34
233	Alaskan Permafrost Groundwater Storage Changes Derived from GRACE and Ground Measurements. 2011 , 3, 378-397		47
232	The effect of fire and permafrost interactions on soil carbon accumulation in an upland black spruce ecosystem of interior Alaska: implications for post-thaw carbon loss. 2011 , 17, 1461-1474		92
231	Assessing the role of differential frost heave in the origin of non-sorted circles. 2011 , 75, 325-333		10
230	Degrading Mountain Permafrost in Southern Norway: Spatial and Temporal Variability of Mean Ground Temperatures, 1999\(\mathbb{\textit{0}}\)009. Permafrost and Periglacial Processes, 2011, 22, 361-377	4.2	71
229	Air and Ground Temperature Variations Observed along Elevation and Continentality Gradients in Southern Norway. <i>Permafrost and Periglacial Processes</i> , 2011 , 22, 343-360	4.2	48
228	The Effects of Snow, Soil Microenvironment, and Soil Organic Matter Quality on N Availability in Three Alaskan Arctic Plant Communities. 2011 , 14, 804-817		64
227	The impact of soil freezing/thawing processes on water and energy balances. 2011 , 28, 169-177		25
226	Soil temperature response to 21st century global warming: the role of and some implications for peat carbon in thawing permafrost soils in North America. 2011 ,		9
225	Soil temperature response to 21st century global warming: the role of and some implications for peat carbon in thawing permafrost soils in North America. 2011 , 2, 121-138		43
224	Modeling the impact of wintertime rain events on the thermal regime of permafrost. 2011 , 5, 945-959		64
223	Multi-scale validation of a new soil freezing scheme for a land-surface model with physically-based hydrology. 2012 , 6, 407-430		84
222	High Arctic Dry Heath CO2 Exchange During the Early Cold Season. 2012 , 15, 1083-1092		11
221	Active layer temperature in two Cryosols from King George Island, Maritime Antarctica. 2012 , 155-156, 12-19		32

(2013-2012)

220	ground conditions. 2012 , 80-81, 136-148	9
219	Airborne electromagnetic imaging of discontinuous permafrost. 2012 , 39, n/a-n/a	107
218	Modeling sub-sea permafrost in the East Siberian Arctic Shelf: The Laptev Sea region. 2012, 117, n/a-n/a	62
217	Permafrost IPhysical Aspects, Carbon Cycling, Databases and Uncertainties. 2012, 159-185	19
216	Soil moisture control over autumn season methane flux, Arctic Coastal Plain of Alaska. 2012 , 9, 1423-1440	63
215	Effects of elevated air temperatures on soil thermal and hydrologic processes in the active layer in an alpine meadow ecosystem of the Qinghai-Tibet Plateau. 2012 , 9, 243-255	6
214	The Effects of Permafrost Thaw on Soil Hydrologic, Thermal, and Carbon Dynamics in an Alaskan Peatland. 2012 , 15, 213-229	143
213	Non-growing season soil CO2 efflux and its changes in an alpine meadow ecosystem of the Qilian Mountains, Northwest China. 2013 , 5, 488-499	8
212	Expert assessment of vulnerability of permafrost carbon to climate change. 2013 , 119, 359-374	212
211	Secondary creep approximations of ice-rich soils and ice using transient relaxation tests. 2013 , 88, 17-36	13
210	Satellite-based modeling of permafrost temperatures in a tundra lowland landscape. 2013 , 135, 12-24	82
209	Modeling the subsurface thermal impact of Arctic thaw lakes in a warming climate. 2013 , 53, 69-79	17
208	Representing permafrost properties in CoLM for the QinghaiRizang (Tibetan) Plateau. 2013, 87, 68-77	38
207	Microbial use of 15N-labelled maize residues affected by winter temperature scenarios. 2013 , 65, 22-32	19
206	The effects of fire on the thermal stability of permafrost in lowland and upland black spruce forests of interior Alaska in a changing climate. 2013 , 8, 035030	85
205	Rapid responses of permafrost and vegetation to experimentally increased snow cover in sub-arctic Sweden. 2013 , 8, 035025	92
204	The active layer: A conceptual review of monitoring, modelling techniques and changes in a warming climate. 2013 , 37, 352-376	50
203	Winter soil respiration during soil-freezing process in a boreal forest in Northeast China. 2013 , 6, 349-357	19

202	Mechanisms leading to enhanced soil nitrous oxide fluxes induced by freezethaw cycles. 2013 , 93, 401-414	93
201	PERMAFROST AND PERIGLACIAL FEATURES Active Layer Processes. 2013 , 421-429	1
200	The Impact of Snow Accumulation on the Active Layer Thermal Regime in High Arctic Soils. 2013 , 12, vzj2012.0058	21
199	Comparison of seasonal soil microbial process in snow-covered temperate ecosystems of northern China. 2014 , 9, e92985	10
198	Process-based isotope partitioning of winter soil respiration in a subalpine ecosystem reveals importance of rhizospheric respiration. 2014 , 121, 389-408	12
197	Characterizing snowmelt anomalies in hydrochemographs of a karst spring, Cumberland Valley, Pennsylvania (USA): evidence for multiple recharge pathways. 2014 , 72, 47-58	10
196	The effect of snow: How to better model ground surface temperatures. 2014 , 102, 63-77	21
195	Dynamics of greenhouse gas formation in relation to freeze/thaw soil depth in a flooded peat marsh of Northeast China. 2014 , 75, 202-210	19
194	A synthesis of methane emissions from 71 northern, temperate, and subtropical wetlands. 2014 , 20, 2183-97	291
193	Influence of Snow, Food, and Rock Cover on Royle Pika Abundance in Western Himalaya. 2014 , 46, 558-567	8
193	Influence of Snow, Food, and Rock Cover on Royle Pika Abundance in Western Himalaya. 2014, 46, 558-567 Reduction of air- and liquid water-filled soil pore space with freezing explains high temperature sensitivity of soil respiration below 0 T.C. 2014, 78, 90-96	18
	Reduction of air- and liquid water-filled soil pore space with freezing explains high temperature	
192	Reduction of air- and liquid water-filled soil pore space with freezing explains high temperature sensitivity of soil respiration below 0 T.C. 2014 , 78, 90-96 Effects of arctic shrub expansion on biophysical vs. biogeochemical drivers of litter decomposition.	18
192	Reduction of air- and liquid water-filled soil pore space with freezing explains high temperature sensitivity of soil respiration below 0 T.C. 2014, 78, 90-96 Effects of arctic shrub expansion on biophysical vs. biogeochemical drivers of litter decomposition. 2014, 95, 1861-75 Impacts of surface soil organic content on the soil thermal dynamics of alpine meadows in	18
192 191 190	Reduction of air- and liquid water-filled soil pore space with freezing explains high temperature sensitivity of soil respiration below 0 T.C. 2014, 78, 90-96 Effects of arctic shrub expansion on biophysical vs. biogeochemical drivers of litter decomposition. 2014, 95, 1861-75 Impacts of surface soil organic content on the soil thermal dynamics of alpine meadows in permafrost regions: data from field observations. 2014, 232-234, 414-425 Active layer thermal regime at different vegetation covers at Lions Rump, King George Island,	18 66 21
192 191 190	Reduction of air- and liquid water-filled soil pore space with freezing explains high temperature sensitivity of soil respiration below OEC. 2014, 78, 90-96 Effects of arctic shrub expansion on biophysical vs. biogeochemical drivers of litter decomposition. 2014, 95, 1861-75 Impacts of surface soil organic content on the soil thermal dynamics of alpine meadows in permafrost regions: data from field observations. 2014, 232-234, 414-425 Active layer thermal regime at different vegetation covers at Lions Rump, King George Island, Maritime Antarctica. 2014, 225, 36-46 Pools, transformations, and sources of P in high-elevation soils: Implications for nutrient transfer to	18 66 21 28
192 191 190 189	Reduction of air- and liquid water-filled soil pore space with freezing explains high temperature sensitivity of soil respiration below Off. 2014, 78, 90-96 Effects of arctic shrub expansion on biophysical vs. biogeochemical drivers of litter decomposition. 2014, 95, 1861-75 Impacts of surface soil organic content on the soil thermal dynamics of alpine meadows in permafrost regions: data from field observations. 2014, 232-234, 414-425 Active layer thermal regime at different vegetation covers at Lions Rump, King George Island, Maritime Antarctica. 2014, 225, 36-46 Pools, transformations, and sources of P in high-elevation soils: Implications for nutrient transfer to Sierra Nevada lakes. 2014, 217-218, 65-73 Long-term anoxia and release of ancient, labile carbon upon thaw of Pleistocene permafrost. 2015,	18 66 21 28

(2016-2015)

184	Noah Modelling of the Permafrost Distribution and Characteristics in the West Kunlun Area, Qinghai-Tibet Plateau, China. <i>Permafrost and Periglacial Processes</i> , 2015 , 26, 160-174	2. 23
183	Permafrost soils and carbon cycling. 2015 , 1, 147-171	176
182	The role of snow cover affecting boreal-arctic soil freezethaw and carbon dynamics. 2015 , 12, 5811-5829	37
181	Uranium isotopes and dissolved organic carbon in loess permafrost: Modeling the age of ancient ice. 2015 , 152, 143-165	22
180	Stoichiometry and temperature sensitivity of methanogenesis and CO2 production from saturated polygonal tundra in Barrow, Alaska. 2015 , 21, 722-37	57
179	Using field observations to inform thermal hydrology models of permafrost dynamics with ATS (v0.83). 2015 ,	5
178	Methane transport from the active layer to lakes in the Arctic using Toolik Lake, Alaska, as a case study. 2015 , 112, 3636-40	41
177	Winter gas exchange between the atmosphere and snow-covered soils on Niwot Ridge, Colorado, USA. 2015 , 8, 677-688	8
176	Presence of rapidly degrading permafrost plateaus in south-central Alaska. 2016, 10, 2673-2692	27
175	A parameterization of respiration in frozen soils based on substrate availability. 2016 , 13, 1991-2001	19
174	Scaling-up permafrost thermal measurements in western Alaska using an ecotype approach. 2016 , 10, 2517-2532	24
173	Shallow snowpack inhibits soil respiration in sagebrush steppe through multiple biotic and abiotic mechanisms. 2016 , 7, e01297	7
172	Permafrost Warming in a Subarctic Peatland I Which Meteorological Controls are Most Important?. Permafrost and Periglacial Processes, 2016 , 27, 177-188	. 31
171	Importance of soil thermal regime in terrestrial ecosystem carbon dynamics in the circumpolar north. 2016 , 142, 28-40	11
170	A simplified de Vries-based model to estimate thermal conductivity of unfrozen and frozen soil. 2016 , 67, 564-572	53
169	Variability in the sensitivity among model simulations of permafrost and carbon dynamics in the permafrost region between 1960 and 2009. 2016 , 30, 1015-1037	83
168	Evidence for nonuniform permafrost degradation after fire in boreal landscapes. 2016 , 121, 320-335	39
167	Winter precipitation and snow accumulation drive the methane sink or source strength of Arctic tussock tundra. 2016 , 22, 2818-33	41

166	Increasing the southern side-slope albedo remedies thermal asymmetry of cold-region roadway embankments. 2016 , 123, 115-120	24
165	Plant functional type affects nitrogen use efficiency in high-Arctic tundra. 2016 , 94, 19-28	23
164	Geophysical estimation of shallow permafrost distribution and properties in an ice-wedge polygon-dominated Arctic tundra region. 2016 , 81, WA247-WA263	45
163	Cold season emissions dominate the Arctic tundra methane budget. 2016 , 113, 40-5	217
162	Active layer and permafrost thermal regime in a patterned ground soil in Maritime Antarctica, and relationship with climate variability models. 2017 , 584-585, 572-585	8
161	Applicability of the ecosystem type approach to model permafrost dynamics across the Alaska North Slope. 2017 , 122, 50-75	43
160	Trapped Greenhouse Gases in the Permafrost Active Layer: Preliminary Results for Methane Peaks in Vertical Profiles of Frozen Alaskan Soil Cores. <i>Permafrost and Periglacial Processes</i> , 2017 , 28, 477-484 ⁴⁻²	10
159	Methane Emission Potential from Freshwater Marsh Soils of Northeast China: Response to Simulated Freezing-Thawing Cycles. 2017 , 37, 437-445	6
158	Nonlinear CO flux response to 7IJyears of experimentally induced permafrost thaw. 2017 , 23, 3646-3666	49
157	Contrasting hydrogeologic responses to warming in permafrost and seasonally frozen ground hillslopes. 2017 , 44, 1803	48
156	Coincident aboveground and belowground autonomous monitoring to quantify covariability in permafrost, soil, and vegetation properties in Arctic tundra. 2017 , 122, 1321-1342	31
155	Persistent Changes to Ecosystems following Winter Road Construction and Abandonment in an Area of Discontinuous Permafrost, Nahanni National Park Reserve, Northwest Territories, Canada. 2017 , 49, 259-276	3
154	Near-shore talik development beneath shallow water in expanding thermokarst lakes, Old Crow Flats, Yukon. 2017 , 122, 1070-1089	27
153	Large CO2 and CH4 emissions from polygonal tundra during spring thaw in northern Alaska. 2017 , 44, 504-513	36
152	Microbial mineralization of cellulose in frozen soils. 2017 , 8, 1154	15
151	Special Global Session and Special Session I Complete Session. 2017 ,	
150	Adsorbed cation effects on unfrozen water in fine-grained frozen soil measured using pulsed nuclear magnetic resonance. 2017 , 142, 42-54	25
149	Ground temperature and permafrost distribution in Hurd Peninsula (Livingston Island, Maritime Antarctic): An assessment using freezing indexes and TTOP modelling. 2017 , 149, 560-571	25

148	Numerical Modeling of the Active Layer Thickness and Permafrost Thermal State Across Qinghai-Tibetan Plateau. 2017 , 122, 11,604-11,620	60
147	Towards improved parameterization of a macroscale hydrologic model in a discontinuous permafrost boreal forest ecosystem. 2017 , 21, 4663-4680	8
146	Time-lapse surface wave monitoring of permafrost thaw using distributed acoustic sensing and a permanent automated seismic source. 2017 ,	25
145	Microbial Community and Functional Gene Changes in Arctic Tundra Soils in a Microcosm Warming Experiment. 2017 , 8, 1741	17
144	Review article: Inferring permafrost and permafrost thaw in the mountains of the Hindu Kush Himalaya region. 2017 , 11, 81-99	65
143	Groundwater flow and heat transport for systems undergoing freeze-thaw: Intercomparison of numerical simulators for 2D test cases. 2018 , 114, 196-218	58
142	Numerical Study on the Multifield Mathematical Coupled Model of Hydraulic-Thermal-Salt-Mechanical in Saturated Freezing Saline Soil. 2018 , 18, 04018064	23
141	Spring photosynthetic onset and net CO uptake in Alaska triggered by landscape thawing. 2018 , 24, 3416-34	13526
140	Combined Geophysical Measurements Provide Evidence for Unfrozen Water in Permafrost in the Adventdalen Valley in Svalbard. 2018 , 45, 7606-7614	22
139	Effects of soil water and heat relationship under various snow cover during freezing-thawing periods in Songnen Plain, China. 2018 , 8, 1325	12
138	Improvements in Measuring Unfrozen Water in Frozen Soils Using the Pulsed Nuclear Magnetic Resonance Method. 2018 , 32, 04017016	11
137	Soil Moisture Controls the Thermal Habitat of Active Layer Soils in the McMurdo Dry Valleys, Antarctica. 2018 , 123, 46-59	13
136	Modelling present and future permafrost thermal regimes in Northeast Greenland. 2018, 146, 199-213	16
135	Infiltration into frozen soil: From core-scale dynamics to hillslope-scale connectivity. 2018 , 32, 66-79	15
134	Using Persistent Scatterer Interferometry to Map and Quantify Permafrost Thaw Subsidence: A Case Study of Eboling Mountain on the Qinghai-Tibet Plateau. 2018 , 123, 2663-2676	23
133	The Improved Freezellhaw Process of a Climate-Vegetation Model: Calibration and Validation Tests in the Source Region of the Yellow River. 2018 , 123, 13,346	6
132	Dependence of C-Band Backscatter on Ground Temperature, Air Temperature and Snow Depth in Arctic Permafrost Regions. 2018 , 10, 142	14
131	The physical properties of coarse-fragment soils and their effects on permafrost dynamics: a case study on the central Qinghailibetan Plateau. 2018 , 12, 3067-3083	8

130	Modeling the role of preferential snow accumulation in through talik development and hillslope groundwater flow in a transitional permafrost landscape. 2018 , 13, 105006	54
129	Reviews and syntheses: Changing ecosystem influences on soil thermal regimes in northern high-latitude permafrost regions. 2018 , 15, 5287-5313	85
128	Variations in near-surface debris temperature through the summer monsoon on Khumbu Glacier, Nepal Himalaya. 2018 , 43, 2698-2714	5
127	A method for calculating unfrozen water content of silty clay with consideration of freezing point. 2018 , 161, 474-481	29
126	GPS Interferometric Reflectometry Reveals Cyclic Elevation Changes in Thaw and Freezing Seasons in a Permafrost Area (Barrow, Alaska). 2018 , 45, 5581-5589	18
125	Detecting the permafrost carbon feedback: talik formation and increased cold-season respiration as precursors to sink-to-source transitions. 2018 , 12, 123-144	36
124	Modeling Long-Term Permafrost Degradation. 2018 , 123, 1756-1771	19
123	Thermal Regime and Properties of Soils and Ice-Rich Permafrost in Beacon Valley, Antarctica. 2018 , 123, 1797-1810	3
122	Liquid-Vapor-Air Flow in the Frozen Soil. 2018 , 123, 7393	21
121	Methane Efflux Measured by Eddy Covariance in Alaskan Upland Tundra Undergoing Permafrost Degradation. 2018 , 123, 2695-2710	23
120	Monitoring changes in unfrozen water content with electrical resistivity surveys in cold continuous permafrost. 2018 , 215, 965-977	26
119	Characteristics of Water-Heat Exchanges and Inconsistent Surface Temperature Changes at an Elevational Permafrost Site on the Qinghai-Tibet Plateau. 2018 , 123, 10,057	30
118	Clumped isotope constraints on equilibrium carbonate formation and kinetic isotope effects in freezing soils. 2018 , 235, 402-430	12
117	Understory vegetation mediates permafrost active layer dynamics and carbon dioxide fluxes in open-canopy larch forests of northeastern Siberia. 2018 , 13, e0194014	13
116	Ground surface temperature and the detection of permafrost in the rugged topography on NE Qinghai-Tibet Plateau. 2019 , 333, 57-68	20
115	Sensitivity of Methane Emissions to Later Soil Freezing in Arctic Tundra Ecosystems. 2019 , 124, 2595-2609	15
114	Exploring Subsurface Temperature Dynamics of Frozen Debris Lobes through Thermal Modeling. 2019 ,	1
113	Experimental study on unfrozen water and soil matric suction of the aeolian sand sampled from Tibet Plateau. 2019 , 164, 102784	5

(2020-2019)

112	Retrieval of Permafrost Active Layer Properties Using Time-Series P-Band Radar Observations. 2019 , 57, 6037-6054	23
111	Insights Into Permafrost and Seasonal Active-Layer Dynamics From Ambient Seismic Noise Monitoring. 2019 , 124, 1798-1816	23
110	New insights into the environmental factors controlling the ground thermal regime across the Northern Hemisphere: a comparison between permafrost and non-permafrost areas. 2019 , 13, 693-707	21
109	Microbial utilization of simple carbon substrates in boreal peat soils at low temperatures. 2019 , 135, 438-448	7
108	A new thermal conductivity model for sandy and peat soils. 2019 , 274, 95-105	17
107	Evaluation of calculation models for the unfrozen water content of freezing soils. 2019 , 575, 976-985	17
106	Frost Heave of Irrigation Canals in Seasonal Frozen Regions. 2019 , 2019, 1-14	3
105	Hydro-thermal behaviors of the ground under different surfaces in the Qinghai-Tibet Plateau. 2019 , 161, 99-106	13
104	Sensitivity of active-layer freezing process to snow cover in Arctic Alaska. 2019 , 13, 197-218	16
103	Improving permafrost physics in the coupled Canadian Land Surface Scheme (v.3.6.2) and Canadian Terrestrial Ecosystem Model (v.2.1) (CLASS-CTEM). 2019 , 12, 4443-4467	15
102	A distributed temperature profiling method for assessing spatial variability in ground temperatures in a discontinuous permafrost region of Alaska. 2019 , 13, 2853-2867	10
101	Cold Regions Engineering 2019. 2019 ,	
100	Permafrost Subsidence Monitoring of Qinghai-Tibet Plateau using Sentinel-1 Data. 2019,	
99	Numerical modeling of two-dimensional temperature field dynamics across non-deforming ice-wedge polygons. 2019 , 161, 115-128	3
98	Shallow ground temperature measurements on the highest volcano on Earth, Mt. Ojos del Salado, Arid Andes, Chile. <i>Permafrost and Periglacial Processes</i> , 2019 , 30, 3-18	16
97	Soil thermal conductivity and its influencing factors at the Tanggula permafrost region on the Qinghailibet Plateau. 2019 , 264, 235-246	36
96	Wildfire-Initiated Talik Development Exceeds Current Thaw Projections: Observations and Models From Alaska's Continuous Permafrost Zone. 2020 , 47, e2020GL087565	8
95	Estimation of Permafrost SOC Stock and Turnover Time Using a Land Surface Model With Vertical Heterogeneity of Permafrost Soils. 2020 , 34, e2020GB006585	3

94	Improving the Noah-MP Model for Simulating Hydrothermal Regime of the Active Layer in the Permafrost Regions of the Qinghai-Tibet Plateau. 2020 , 125, e2020JD032588		10
93	Lake outburst accelerated permafrost degradation on Qinghai-Tibet Plateau. 2020 , 249, 112011		29
92	Small-Baseline Approach for Monitoring the Freezing and Thawing Deformation of Permafrost on the Beiluhe Basin, Tibetan Plateau Using TerraSAR-X and Sentinel-1 Data. 2020 , 20,		7
91	Permafrost Mapping with Electrical Resistivity Tomography: A Case Study in Two Wetland Systems in Interior Alaska. 2020 , 25, 199-209		3
90	In-Situ Monitoring and Characteristic Analysis of Freezing-Thawing Cycles in a Deep Vadose Zone. 2020 , 12, 1261		2
89	Active Layer Thickness Retrieval Over the Qinghai-Tibet Plateau Using Sentinel-1 Multitemporal InSAR Monitored Permafrost Subsidence and Temporal-Spatial Multilayer Soil Moisture Data. 2020 , 8, 84336-84351		9
88	Pore-scale controls on hydrological and geochemical processes in peat: Implications on interacting processes. 2020 , 207, 103227		21
87	Biogeochemical Cycling of Redox-Sensitive Elements in Permafrost-Affected Ecosystems. 2020 , 245-265		5
86	Sensitivity of soil freeze/thaw dynamics to environmental conditions at different spatial scales in the central Tibetan Plateau. 2020 , 734, 139261		7
85	Response of soil water content and temperature to rangeland desertification in an alpine region with seasonally frozen soil and plateau pika (Ochotona curzoniae) burrows. 2020 , 20, 3722-3732		0
84	Snow depths' impact on soil microbial activities and carbon dioxide fluxes from a temperate wetland in Northeast China. 2020 , 10, 8709		3
83	Groundwater as a major source of dissolved organic matter to Arctic coastal waters. 2020 , 11, 1479		36
82	Development of a Shallow-Depth Soil Temperature Estimation Model Based on Air Temperatures and Soil Water Contents in a Permafrost Area. 2020 , 10, 1058		3
81	The Combination of Wildfire and Changing Climate Triggers Permafrost Degradation in the Khentii Mountains, Northern Mongolia. 2020 , 11, 155		7
80	Ground temperature and snow depth variability within a subarctic peat plateau landscape. Permafrost and Periglacial Processes, 2020, 31, 255-263 4	.2	5
79	Impacts of Degrading Ice-Wedges on Ground Temperatures in a High Arctic Polar Desert System. 2020 , 125, e2019JF005173		5
78	Review of algorithms and parameterizations to determine unfrozen water content in frozen soil. 2020 , 368, 114277		28
77	Soil thermal regime alteration under experimental warming in permafrost regions of the central Tibetan Plateau. 2020 , 372, 114397		8

(2013-2020)

76	Potential Use of Time-Lapse Surface Seismics for Monitoring Thawing of the Terrestrial Arctic. 2020 , 10, 1875	2
75	On determination method of thermal conductivity of soil solid material. 2020 , 60, 218-228	4
74	Thermal effect of thermokarst lake on the permafrost under embankment. 2021 , 12, 76-82	2
73	Plant E nvironment Interactions in the Low Arctic Torngat Mountains of Labrador. 2021 , 24, 1038-1058	6
72	Simulation of the Present and Future Projection of Permafrost on the Qinghai-Tibet Plateau with Statistical and Machine Learning Models. 2021 , 126, e2020JD033402	20
71	Coupling analysis of the heat-water dynamics and frozen depth in a seasonally frozen zone. 2021 , 593, 125603	57
70	Advancing hydrological process understanding from long-term resistivity monitoring systems. 2021 , 8, e1513	7
69	Geophysical Observations of Taliks Below Drained Lake Basins on the Arctic Coastal Plain of Alaska. 2021 , 126, e2020JB020889	4
68	Active layer thickness as a function of soil water content. 2021 , 16, 055028	10
67	Ecosystem Scale Implication of Soil CO2 Concentration Dynamics During Soil Freezing in Alaskan Arctic Tundra Ecosystems. 2021 , 126, e2020JG005724	О
66	Geofysiske metoder kan fortelle oss hvordan de frosne landomrdene i Arktis tiner. 2021 , 145, 148-159	
65	. 2021, 2,	3
64	Projecting Permafrost Thaw of Sub-Arctic Tundra With a Thermodynamic Model Calibrated to Site Measurements. 2021 , 126, e2020JG006218	3
63	Inferring Permafrost Active Layer Thermal Properties From Numerical Model Optimization. 2021 , 48, e2021GL093306	1
62	Integrating observations and models to determine the effect of seasonally frozen ground on hydrologic partitioning in alpine hillslopes in the Colorado Rocky Mountains, USA. 2021 , 35, e14374	1
61	Do Growth Kinetics of Snow-mold Fungi Explain Exponential CO2 Fluxes Through the Snow?. 2013 , 245-253	1
60	Permafrost Carbon Quantities and Fluxes. 2020 , 179-274	1
59	Rock Glacier Degradation and Instabilities in the European Alps: A Characterisation and Monitoring Experiment in the Turtmanntal, CH. 2013 , 5-13	13

58	PERIGLACIAL LANDFORMS Active Layer Processes. 2007, 2138-2147	5
57	Visualizing cation treatment effects on frozen clay soils through IT scanning. 2020, 175, 103085	4
56	Permafrost active layer. 2020 , 208, 103301	9
55	Circumpolar permafrost maps and geohazard indices for near-future infrastructure risk assessments. 2019 , 6, 190037	31
54	Shallow soils are warmer under trees and tall shrubs across Arctic and Boreal ecosystems. 2021 , 16, 015001	12
53	Characterizing Subzero-Temperature Thermal Properties of Seasonally Frozen Soil in Alpine Forest in the Western Sichuan Province, China. 2016 , 08, 583-593	3
52	A parameterization of respiration in frozen soils based on substrate availability.	2
51	Exploring the sensitivity of soil carbon dynamics to climate change, fire disturbance and permafrost thaw in a black spruce ecosystem.	5
50	Thermal signal propagation in soils in Romania: conductive and non-conductive processes. 2007 , 3, 637-645	10
49	Thermal signal propagation in soils in Romania: conductive and non-conductive processes.	2
48	Evaluation of the ground surface Enthalpy balance from bedrock temperatures (Livingston Island, Maritime Antarctic). 2009 , 3, 133-145	18
47	Transient thermal effects in Alpine permafrost.	1
46	Modeling the impact of wintertime rain events on the thermal regime of permafrost.	12
45	Multi-scale validation of a new soil freezing scheme for a land-surface model with physically-based hydrology.	1
44	Experimental Soil Warming and Permafrost Thaw Increase CH4 Emissions in an Upland Tundra Ecosystem. 2021 , 126, e2021JG006376	1
43	Carbon Dioxide and Methane Release Following Abrupt Thaw of Pleistocene Permafrost Deposits in Arctic Siberia. 2021 , 126,	1
42	Ground Temperature Responses to Climatic Trends in a Range of Surficial Deposits near Kangiqsualujjuaq, Nunavik. 2021 ,	1
41	The climate envelope of Alaska's northern treelines: implications for controlling factors and future treeline advance. 2021 , 44, 1710	5

40	Response of peat-rich permafrost to a warming climate on the northeast Tibetan Plateau. 2021 , 311, 108681	О
39	Evaluation of the ground surface Enthalpy balance from bedrock shallow borehole temperatures (Livingston Island, Maritime Antarctic).	
38	Frozen soil parameterization in a distributed biosphere hydrological model.	
37	Potentials of Applying Surface-Wave Methods for Imaging Subsurface Properties in Permafrost Soils. 2012 ,	
36	The Thermal Regime of Permafrost Regions. 2014 , 239-267	
35	The role of snow cover and soil freeze/thaw cycles affecting boreal-arctic soil carbon dynamics.	1
34	Elastic properties as indicators of heat flux into cold near-surface Arctic sediments. 2020 , 85, MR309-MR323	1
33	The Role of Ground Ice. 2020 , 107-177	O
32	The role of peat on permafrost thaw based on field observations. 2022 , 208, 105772	3
31	Soil enzymes are preferentially associated with larger particles in highly organic Arctic tundra soils. 2021 , 9,	1
30	The Energy Balance of Permafrost Soils and Ecosystems. 2020 , 51-106	
29	Influence of Rainfall Changes on the Temperature Regime of Permafrost in Central Yakutia. 2021 , 10, 1230	1
28	Establishment and Verification of a Thermal Calculation Model Considering Internal Heat Transfer of Accumulated Water in Permafrost Regions. 2021 , 9,	0
27	Tensile behaviors of frozen subgrade soil. 2022 , 81, 1	O
26	Seasonal Fluctuations in Iron Cycling in Thawing Permafrost Peatlands 2022,	О
25	Convective heat transfer of spring meltwater accelerates active layer phase change in Tibet permafrost areas. 2022 , 16, 825-849	O
24	The importance of freezethaw cycles for lateral tracer transport in ice-wedge polygons. 2022 , 16, 851-862	
23	Different responses of surface freeze and thaw phenology changes to warming among Arctic permafrost types. 2022 , 272, 112956	O

22	Overview: Recent advances in the understanding of the northern Eurasian environments and of the urban air quality in China la Pan-Eurasian Experiment (PEEX) programme perspective. 2022 , 22, 4413-4469	1
21	Synthesis of physical processes of permafrost degradation and geophysical and geomechanical properties of permafrost. 2022 , 198, 103522	Ο
20	High nitrate variability on an Alaskan permafrost hillslope dominated by alder shrubs. 2022 , 16, 1889-1901	1
19	Sub-aerial talik formation observed across the discontinuous permafrost zone of Alaska. 2022 , 15, 475-481	3
18	Probabilistic estimation of depth-resolved profiles of soil thermal diffusivity from temperature time series. 2022 , 10, 687-704	0
17	A repository of measured soil freezing characteristic curves: 1921 to 2021. 2022 , 14, 3365-3377	Ο
16	Frozen soil hydrological modeling for a mountainous catchment northeast of the Qinghaillibet Plateau. 2022 , 26, 4187-4208	0
15	Permafrost thaw drives surface water decline across lake-rich regions of the Arctic.	1
14	Multi-year observations reveal a larger than expected autumn respiration signal across northeast Eurasia. 2022 , 19, 4779-4799	0
13	Impact of tundra vegetation type on topsoil temperature in central Spitsbergen (Svalbard, High Arctic). 2022 , 116196	1
12	Ground Surface Displacement After a Forest Fire Near Mayya, Eastern Siberia, Using InSAR: Observation and Implication for Geophysical Modeling. 2022 , 9,	0
11	Himalayan alpine ecohydrology: An urgent scientific concern in a changing climate.	O
10	Water and heat coupling processes and its simulation in frozen soils: Current status and future research directions. 2023 , 222, 106844	0
9	Using atmospheric observations to quantify annual biogenic carbon dioxide fluxes on the Alaska North Slope. 2022 , 19, 5953-5972	1
8	Quantitative Impact of Organic Matter and Soil Moisture on Permafrost.	0
7	Effects of soil parameterization on permafrost modeling in the Qinghai-Tibet Plateau: A calibration-constrained analysis. 2023 , 210, 103833	O
6	Burning trees in frozen soil: Simulating fire, vegetation, soil, and hydrology in the boreal forests of Alaska. 2023 , 481, 110367	О
5	The effects of temperature on shallow borehole NMR measurements in permafrost. 2023 , 211, 103850	O

CITATION REPORT

4	Dynamics of the freezethaw front of active layer on the Qinghai-Tibet Plateau. 2023 , 430, 116353	Ο
3	Permafrost Thermal Responses to Asymmetrical Climate Changes: An Integrated Perspective. 2023 , 50,	O
2	Investigating ten years of warming and enhanced snow depth on nutrient availability and greenhouse gas fluxes in a High Arctic ecosystem. 2023 , 55,	O
1	Winter temperature and growing season CO₂ budgets of deciduous needle leaf forest in eastern Siberia. 2023 , 53, 20-24	0